

Pluripotency-related, Valproic Acid (VPA)-induced Genome-wide Histone H3 Lysine 9 (H3K9) Acetylation Patterns in Embryonic Stem Cells^{*[5]}

Received for publication, May 31, 2011, and in revised form, July 27, 2011. Published, JBC Papers in Press, August 17, 2011, DOI 10.1074/jbc.M111.266254

Hadas Hezroni¹, Badi Sri Sailaja¹, and Eran Meshorer²

From the Department of Genetics, the Institute of Life Sciences, Hebrew University of Jerusalem, Edmond J. Safra Campus, Jerusalem 91904, Israel

Background: Embryonic stem cell (ESC) chromatin is characterized by a unique set of histone modifications, including enrichment for H3K9ac. Recent studies suggest that HDAC inhibitors (HDACi) promote pluripotency.

Results: Using H3K9ac ChIP-seq analyses and gene expression in E14 mouse ESCs before and after treatment with a low level of the HDACi valproic acid (VPA), we show that H3K9ac is enriched at gene promoters and is highly correlated with gene expression and with various genomic features, including different active histone marks and pluripotency-related transcription factors.

Conclusion: This study provides insights into the genomic response of ESCs to low level HDACi, which leads to increased pluripotency. The results suggest that a mild (averaging less than 40%) but global change in the chromatin state is involved in increased pluripotency and that specific mechanisms operate selectively in bivalent genes to maintain constant H3K9ac levels. Our data support the notion that H3K9ac has an important role in ESC biology.

Significance: Understanding the mechanisms that improve and support pluripotency of ESCs, such as the use of the HDAC inhibitor VPA, will promote intelligent manipulation of ESCs and expedite their use in the clinic.

Embryonic stem cell (ESC) chromatin is characterized by a unique set of histone modifications, including enrichment for H3 lysine 9 acetylation (H3K9ac). Recent studies suggest that histone deacetylase (HDAC) inhibitors promote pluripotency. Here, using H3K9ac ChIP followed by high throughput sequencing analyses and gene expression in E14 mouse ESCs before and after treatment with a low level of the HDAC inhibitor valproic acid, we show that H3K9ac is enriched at gene promoters and is highly correlated with gene expression and with various genomic features, including different active histone marks and pluripotency-related transcription factors. Curiously, it predicts the cellular location of gene products. Treatment of ESCs with valproic acid leads to a pervasive genome-wide and time-dependent increase in H3K9ac, but this increase is selectively suppressed after 4 h in H3K4me3/H3K27me3 bivalent genes. H3K9ac increase is dependent on the promoter's chromatin state and is affected by the binding of P300, various transcription factors, and active histone marks. This study provides insights into the genomic response of ESCs to a low level of HDAC inhibitor, which leads to increased pluripotency. The results suggest that a mild (averaging less than 40%) but global change in the chromatin state is involved in increased pluripotency and that specific mechanisms operate selectively in biva-

lent genes to maintain constant H3K9ac levels. Our data support the notion that H3K9ac has an important role in ESC biology.

Embryonic stem cell (ESC)³ chromatin is characterized by several features that distinguish it from that of differentiated cells and enable the cells to maintain their pluripotent nature (1). Aside from the hyperdynamic and loose nature of chromatin architectural proteins (2) and the fewer, larger, and less condensed heterochromatin domains (3–5), the ESC chromatin is characterized by a unique histone modification pattern (6). Generally, the ESC chromatin is enriched for histone modifications associated with transcriptional activation, such as acetylations of histones H3 and H4 (7), trimethylations of H3K4 and H3K36, and dimethylation of H3K36 (4). In addition, developmental genes in ESCs, termed “bivalent” genes, are marked by both active histone marks (*i.e.* trimethylated H3K4 and the repressive mark trimethylated H3K27) (8, 9). Such domains tend to be located at the promoters of genes that are not expressed in ESCs and are thought to function in the silencing of developmental genes while keeping them poised for activation.

The level of histone acetylation is mediated by the activity of both histone acetyltransferases (HATs), which acetylate lysine

* This work was supported in part by the Edmond J. Safra Foundation.

[5] The on-line version of this article (available at <http://www.jbc.org>) contains supplemental Tables S1 and S2 and Figs. S1–S9.

¹ An Edmond J. Safra Fellow.

² A Joseph H. and Belle R. Braun Senior Lecturer in Life Sciences, supported by Israel Science Foundation Grants 215/07 and 943/09, Israel Ministry of Health Grant 6007, European Union Grants IRG-206872 and 238176, the Israel Cancer Research Foundation, and the Internal Applicative Medical Grants of the Hebrew University. To whom correspondence should be addressed. E-mail: meshorer@huji.ac.il.

³ The abbreviations used are: ESC, embryonic stem cell; H3K4, H3K9, H3K27, and H3K36, histone H3 lysine 4, 9, 27, and 36, respectively; H3K9ac and H3K27ac, H3K9 and H3K27 acetylation, respectively; H3K4me1 and H3K4me2, methylated and dimethylated H3K4, respectively; H3K4me3, H3K9me3, H3K27me3, and H3K36me3, trimethylated H3K4, H3K9, H3K27, and H3K36, respectively; HAT, histone acetyltransferase; HDAC, histone deacetylase; EB, embryoid body; VPA, valproic acid; MEF, mouse embryonic fibroblast; ChIP-seq, ChIP followed by high throughput sequencing; TF, transcription factor; GO, gene ontology; NPC, neuronal progenitor cell.

residues of the N-terminal histone tails, and histone deacetylases (HDACs), which deacetylate these residues. Histone acetylation is involved in the regulation of diverse cellular processes, including nucleosome assembly, chromatin folding, and transcriptional regulation (10). Several studies published in the past several years have demonstrated the importance of adequate histone acetylation levels during development and particularly in ESC biology. First, HDAC1 knock-out mice die before embryonic day E10.5 (11), HDAC1 knock-out ESCs show reduced proliferation and histone hyperacetylation (11), and HDAC1 conditional knock-out ESCs show enhanced differentiation when induced to form embryoid bodies (EBs) (12). Second, low levels of HDAC inhibitors are able to increase pluripotency and support self-renewal in ESCs (13–15), whereas higher levels of HDAC inhibitors accelerate ESC differentiation (16, 17). More specifically, the HDAC inhibitor valproic acid (VPA) has been reported to improve the reprogramming efficiency of somatic cells into induced pluripotent stem cells in both mouse and human cells (18, 19). Third, the levels of H3 lysine 9 acetylation (H3K9ac) have been reported to be enriched in mouse and human ESCs compared with differentiated cells (4, 20) and to be globally reduced during endoderm-like differentiation of human ESCs (21). Finally, we recently showed that different HDAC inhibitors can restore pluripotency of the mouse ESC line E14, which has reduced H3K9 acetylation levels and a diminished potential to reprogram mouse embryonic fibroblasts (MEFs) when compared with other ESC lines (13). HDAC inhibition increased the pluripotency of E14 in conjunction with increased H3K9 acetylation levels to levels comparable with other ESC lines.

To gain more insight into the molecular mechanisms that underlie the association between pluripotency and H3K9 acetylation level and the increase in pluripotency and reprogramming capacity following HDAC inhibition, we assayed global gene expression and H3K9 acetylation state before and after treatment with a low level of VPA. We find that HDAC inhibition leads to a mild (averaging less than 40%) but global increase in H3K9 acetylation level in gene promoters, which is not accompanied by a global transcriptional activation. We also show that the increase in acetylation level is dependent on the chromatin state and correlates with the binding of P300 and various transcription factors and active histone marks.

EXPERIMENTAL PROCEDURES

Data Source—In this paper, we analyzed the results of gene expression microarrays and H3K9ac chromatin immunoprecipitation (ChIP) followed by high throughput sequencing (ChIP-seq) in E14 mouse ESCs before and after 4 or 16 h of VPA treatments that we have previously performed (13). All sequencing and expression data have been deposited in the Gene Expression Omnibus (GEO) data repository under accession number GSE23958.

Microarray Analysis—Data were normalized with the robust multiarray average method, using Affymetrix Expression Console version 1.1. Genes were defined as differentially expressed if they showed a 1.5-fold or higher change in expression level in each of the two independent repeats, between the VPA-treated cells and the corresponding untreated cells.

ChIP-seq Analysis—50-bp reads generated by the SOLiD sequencer were aligned to the UCSC mm9 assembly of the mouse genome using Bowtie software, version 0.12.5 (22), allowing for up to two mismatches. Only uniquely aligned reads were further analyzed. Genomic regions significantly enriched for H3K9ac were identified using CCAT (23), with a sliding window of 500 bp, an enrichment score cut-off of 3.0, and an FDR cut-off of 0.05. Intersections between the enriched regions of the three samples or between enriched regions to different genomic features (promoters, exons, and introns) were found using Galaxy (24). Read density heat maps of H3K9ac, H3K27ac, H3K4me2, H3K4me3, and H3K27me3 around known transcriptional start sites (TSS) and enrichment values for each gene were calculated and generated using SeqMiner (25). Average ChIP enrichment signals over known TSSs were calculated and visualized using CEAS (26).

Public Data Sources and Analysis—ChIP-seq data sets of histone modifications were downloaded from GEO under the following accession numbers: GSM281695 (H3K4me1), GSM281694 (H3K4me2), GSM307618 (H3K4me3), GSM307620 (H3K36me3), GSM307619 (H3K27me3), GSM307621 (H3K9me3), GSM307617 (ESC whole cell extract), and GSM594578 (H3K27ac) (27–29). For H3K27ac, raw reads were downloaded and aligned to the UCSC mm9 assembly of the mouse genome using Bowtie software, version 0.12.5 (22), allowing for up to two mismatches. For the other histone modifications, aligned reads were downloaded and converted from mm8 to mm9 using Galaxy lift-over. Genomic regions enriched for H3K4me1, H3K4me3, H3K27me3, H3K36me, and H3K9me3 compared with whole cell extract sample were identified using MACS (30) with a *p* value cut-off of 1×10^{-5} . P300 binding sites were downloaded (27) and converted from mm8 to mm9 using Galaxy lift-over. To compare H3K9ac levels in selected genomic regions between the three ESCs lines used in these previous studies (E14, V6.5, and R1 mouse ESCs), we performed ChIP-real-time PCR for H3K9ac for two genic regions and one intergenic region and found that H3K9ac levels were comparable between the three different lines (supplemental Fig. S1). To further validate increased H3K9ac following VPA, we also compared these same regions in E14 ESCs before and after 16 h of VPA treatment and found an excellent agreement with the ChIP-seq data (supplemental Fig. S1).

Cell Culture—Primary mouse embryonic fibroblasts (MEFs) were grown with Dulbecco's modified Eagle's medium (DMEM; Sigma) supplemented with 10% fetal bovine serum (FBS; Biological Industries), 100 units/ml penicillin, and 0.1 mg/ml streptomycin (Biological Industries), and 2 mM L-glutamine (Biological Industries). To prevent proliferation, MEFs were treated with 10 $\mu\text{g}/\mu\text{l}$ mitomycin C (Holland-Moran) for 3 h. MEFs were maintained at 37 °C, 5% CO₂. We used three mouse ESC lines: R1, V6.5, and E14tg2a (E14) cells, all available at ATCC. All ESCs were grown on a feeder layer of mitomycin C-treated MEFs on 0.2% gelatin-coated cell culture dishes. Culture medium consisted of DMEM, 15% ES-grade fetal calf serum (FCS, Biological Industries), 1 mM sodium pyruvate (Biological Industries), 0.1 mM nonessential amino acids (Biological Industries), 0.1 mM β -mercaptoethanol (Sigma), 100 units/ml penicillin, and 0.1 mg/ml streptomycin and 1000 units/ml leu-

kemia inhibitory factor. ESCs were maintained at 37 °C, 5% CO₂ and fed with fresh media every day. For differentiation, ESCs were plated on bacterial culture dishes without leukemia inhibitory factor for 4 days to allow for EB formation. EBs were replated on tissue culture plates coated with poly-L-ornithine (Sigma) and fibronectin (R&D Systems) in DMEM/F-12 medium (Sigma) supplemented with ITS (5 mg/ml insulin, 50 mg/ml transferrin, 30 nM selenium chloride; Invitrogen) and 5 mg/ml fibronectin. For HDAC inhibitor treatment, cells were grown in the presence of VPA (catalog no. P4543, Sigma) at a final concentration of 0.5 mM for either 4 or 16 h.

Pathway Activity Analysis—Changes in pathway activity during ESC differentiation were analyzed using an algorithm that evaluates the interaction structure across predefined canonical networks (31). In order to score the activity of a certain pathway, the algorithm evaluates the status of all of the input genes of each interaction in the pathway (based on microarray data) and determines the probability of the materialization of the interaction as the joint probabilities of all input genes. The final activity score of a pathway is an average of the scores of all interactions. This algorithm was applied to a data set of gene expression of three different mouse ESC lines at 11 time points during the differentiation into EBs (34) in order to score the activity and consistency of 288 known pathways indexed in the Pathway Interaction Database (33).

RESULTS

H3K9ac Is Enriched at Promoters and Correlates with Gene Expression Levels—To determine the genomic distribution pattern of acetylated H3K9 in E14 mouse ESCs, we performed ChIP-seq of H3K9ac using SOLiD sequencing. The read density spanning 5 kb of TSSs of 20,500 genes from the Refseq database was compared with that of another histone acetylation, H3K27ac (27), and with known promoter-associated histone marks, including H3K4me2, H3K4me3, and H3K27me3 (28, 29). *k*-Means clustering of the TSS regions and heat map visualization were performed using seqMINER (25). These analyses revealed an enrichment of H3K9ac at the TSS regions of almost half of the genes (Fig. 1A). H3K9ac signal at these regions highly correlated with that of H3K27ac, H3K4me2, and H3K4me3 (Fig. 1A). Genes that were marked by both H3K4me3 and H3K27me3 (bivalent genes) had very low levels of H3K9ac. Both the read density heat map and the average profile at the region spanning 3 kb of TSSs (Fig. 1B) showed two major peaks of H3K9ac near the TSS, one 500 bp upstream and one 500 bp downstream of the TSS. In addition, high correlation was observed between H3K9 acetylation level and gene expression level, measured using Affymetrix gene expression microarrays ($R^2 = 0.695$) (Fig. 1C), in agreement with the presence of H3K9ac in promoters of active genes occupied by activating transcription factors (TFs) (10).

Low Level VPA Treatment Leads to a Global Increase in H3K9ac—To identify the genes and genomic regions that are associated with increased pluripotency of E14 mouse ESCs following HDAC inhibition, we also performed ChIP-seq for H3K9ac in E14 cells treated with 0.5 mM VPA for either 4 or 16 h. Genomic regions significantly enriched for H3K9ac compared with the input sample were identified using CCAT (23)

for each of the three samples. The number of identified regions significantly increased after both 4 and 16 h of VPA treatment, at different chromosomes and genomic features, implying a global increase in acetylation of H3K9 following HDAC inhibition (Fig. 1D and supplemental Fig. S2). In addition, the average profile at the region spanning 3 kb of TSSs also significantly increased after the treatments, implying an increase in H3K9ac at promoter regions (Fig. 1B). Interestingly, microarray analyses of gene expression before and after VPA treatment showed that the treatment had almost no effect on expression levels, despite the increased H3K9 acetylation levels at promoter regions (supplemental Fig. S3, A and B). After 4 h of VPA treatment, 77 genes were up-regulated and 26 were down-regulated, whereas after 16 h, 39 genes were up-regulated and 37 were down-regulated (supplemental Table S1). One of the genes that were down-regulated after 16 h was KAT2B, an H3 lysine acetyltransferase and a member of several transcriptional activators. This might explain the decrease in the number of up-regulated genes between 4 and 16 h.

To calculate a single H3K9 acetylation enrichment value for each gene, the number of reads at each promoter (defined as the region between 1 kb upstream and 1 kb downstream of the TSS) was counted and normalized to the input sample using seqMINER (25). Comparison of the treated and untreated samples revealed that the acetylation level of H3K9 increased only mildly (*i.e.* averaging less than 20 and 40% for the 4 and 16 h time points, respectively) but across almost the entire set of genes (Fig. 1, A and B). In addition, we found that the response to VPA was different for promoters with different initial acetylation levels. Although the HDAC inhibition hardly had any effect on promoters that were not acetylated before the treatment (enrichment value of around 0), the treatment significantly increased the acetylation level of H3K9 at promoters that were acetylated at intermediate level (enrichment value of around 1.5). In genes that were initially highly acetylated (enrichment value larger than 3), the acetylation level decreased after 4 h and did not change significantly after 16 h (Fig. 2, A–D, and supplemental Fig. S4). The distribution of change in acetylation level was significantly higher after 16 h of VPA treatment than after 4 h ($p \ll 10^{-10}$, two-tailed *t* test) (Fig. 2E), indicating that the effect of VPA treatment on H3K9 acetylation level is larger after 16 h. The different response to HDAC inhibition in different genes might result from a different chromatin state, which either supports or prevents recruitment of various chromatin-modifying enzymes, such as HATs.

Sensitivity to DNase I and Binding by P300 Affect the Response to HDAC Inhibition—In order to characterize the chromatin state of genes with different initial H3K9 acetylation levels, we compared the initial acetylation level with a genome-wide map of sites that are hypersensitive to DNase I digestion, previously generated for mouse ESCs using DNase-seq (35). Promoters that were highly acetylated on H3K9 overlapped with sites that are highly sensitive to DNase I digestion (Fig. 3A), indicating an open chromatin conformation at the promoters of these genes. Moreover, the increase in acetylation level following VPA treatment was higher for genes with higher DNase I hypersensitivity scores (Fig. 3B), indicating that open

VPA-induced Genome-wide H3K9ac Patterns in ESCs

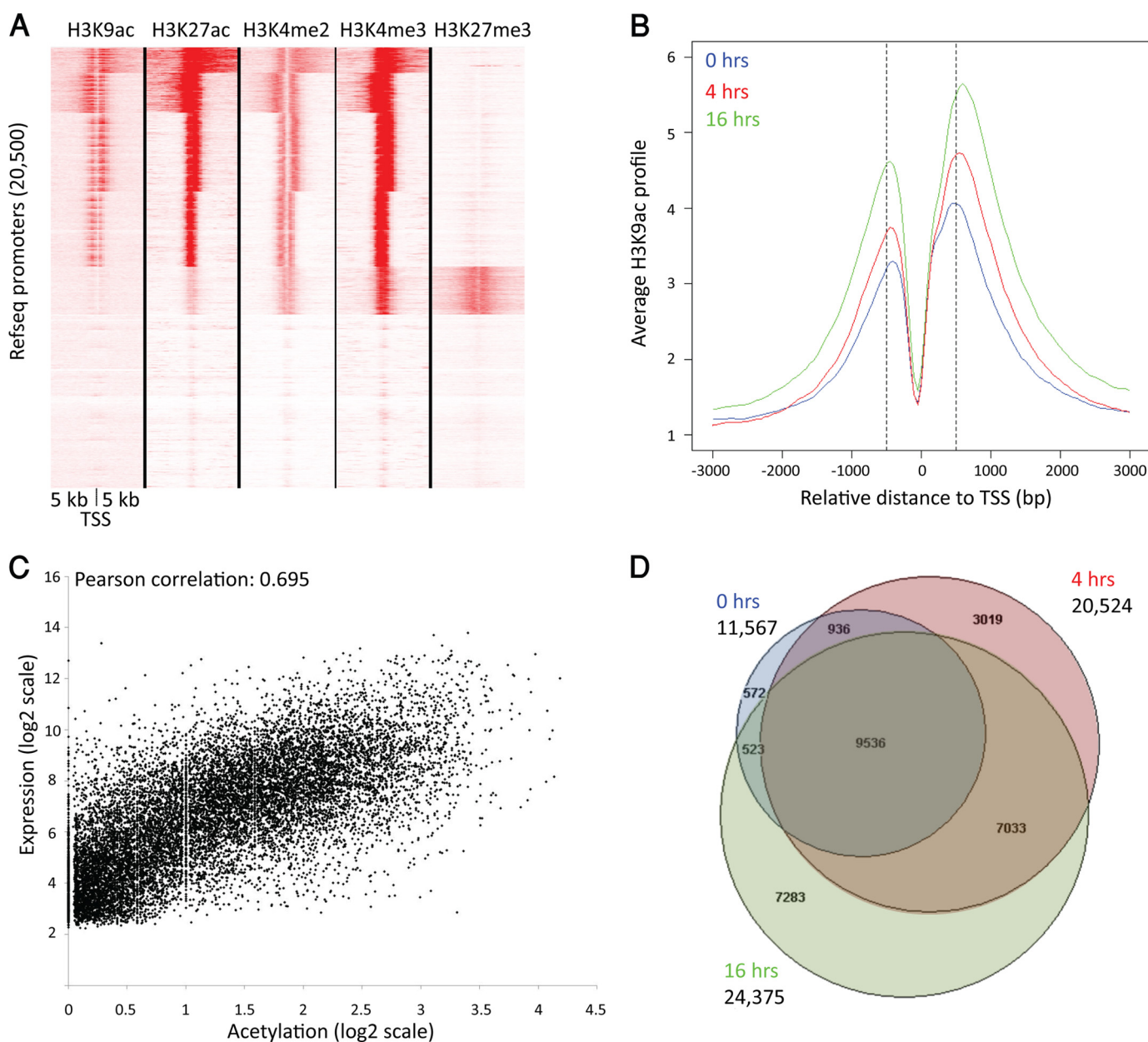


FIGURE 1. Genome-wide mapping of H3K9ac in ESCs before and after VPA treatment. *A*, tag densities of H3K9ac, H3K27ac, H3K4me2, H3K4me3, and H3K27me3 in a window of 10 kb around a set of 20,500 TSSs of known genes from the Refseq database. *k*-Means clustering and generation of heat map were performed using seqMINER. *B*, average ChIP enrichment signals over regions spanning 6 kb around TSSs, calculated and visualized using CEAS, for cells treated with VPA for 0, 4, or 16 h. *Dashed lines* are positioned at -500 and $+500$ bp relative to the TSS. *C*, correlation between H3K9ac level at gene promoters and their corresponding expression level. Acetylation level was calculated using seqMINER for each promoter, defined as the region between 1 kb upstream and 1 kb downstream of the TSS, and presented in log₂ scale. Expression level was measured using Affymetrix gene expression microarrays and is the average between two independent repeats. *D*, Venn diagram presenting the overlap between genomic regions enriched for H3K9ac in cells treated with VPA for 0, 4, or 16 h.

chromatin increases the potential of promoters to undergo increased acetylation after HDAC inhibition. Promoters that were associated with the top 10% of DNase I-hypersensitive sites showed a significant increase in H3K9 acetylation even at low initial acetylation levels (supplemental Fig. S5A). This suggests that the acetylation level of most genes with low initial acetylation levels does not increase after HDAC inhibition, probably due to a condensed chromatin structure. On the contrary, promoters that did not overlap with any DNase I-hypersensitive sites showed a significant decrease in acetylation after the treatment (Fig. 3B and supplemental Fig. S5B). To test whether the recruitment of a specific HAT, P300, affects the

response of different genes to HDAC inhibition, we compared the acetylation level of H3K9 before and after the treatments with a genome-wide map of P300 binding sites, previously generated for mouse ESCs using ChIP-seq (27). The percentage of genes whose promoter regions overlapped with P300 peaks increased from 6% for genes that were not H3K9-acetylated to 71% for genes with a high H3K9 acetylation level (Fig. 3C). This suggests that P300 has a role in acetylating H3K9 in gene promoters in mouse ESCs.

Binding by P300 also affected the potential of a given promoter to be hyperacetylated following VPA treatment; the distribution of change in acetylation level was significantly higher

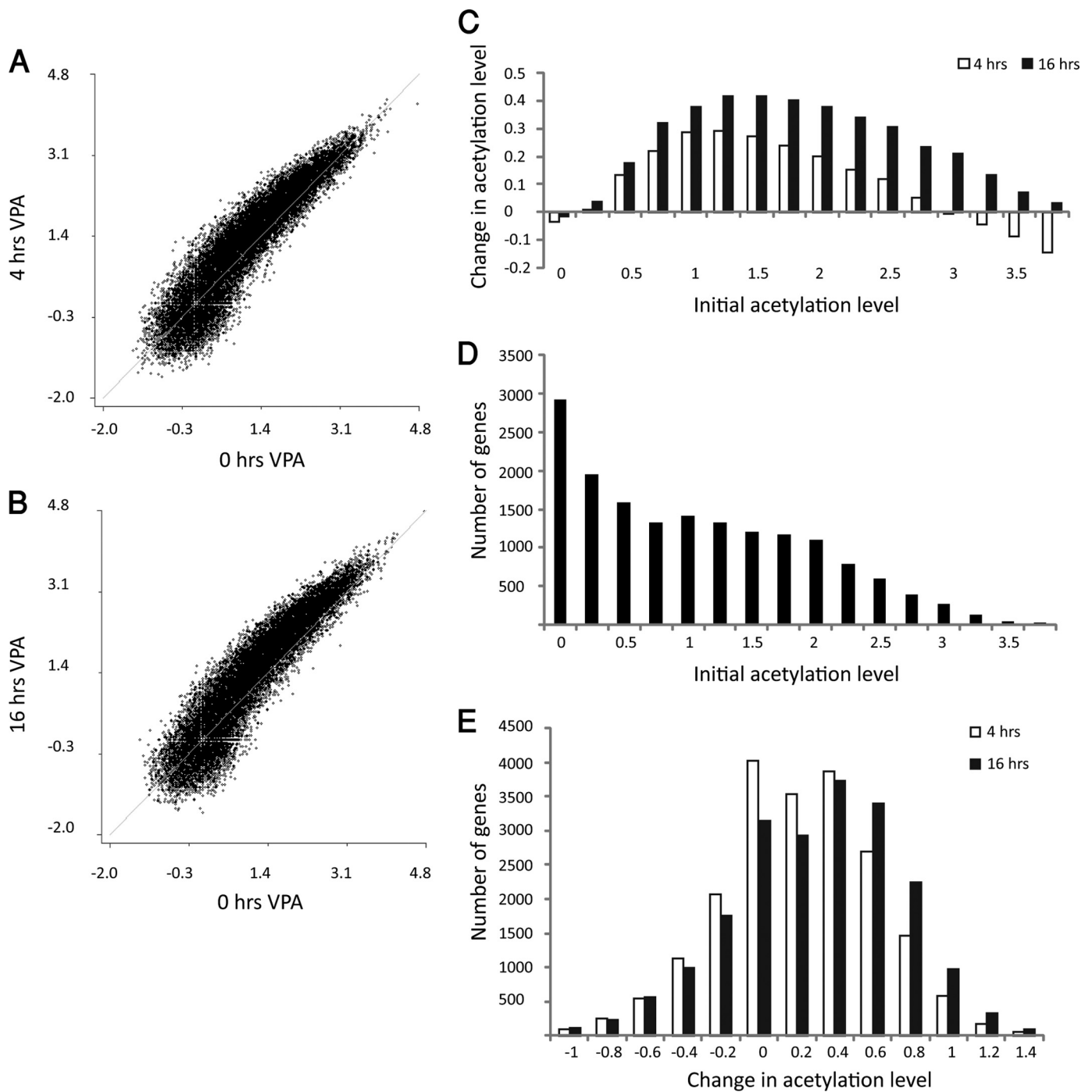


FIGURE 2. Response to VPA treatment is dependent on initial acetylation level. *A* and *B*, correlation between H3K9ac enrichment scores of 20,500 promoters in untreated E14 cells and E14 treated with VPA for either 4 h (*A*) or 16 h (*B*). Enrichment scores are presented in log₂ scale. *C*, genes were divided into 16 groups based on their initial H3K9 acetylation level. The average change in acetylation enrichment score after either 4 or 16 h of VPA treatment was calculated for each group. Only genes with initial enrichment scores larger than 0 are presented. *D*, the number of genes in each initial H3K9 acetylation level. *E*, distribution of genes according to the change in H3K9 acetylation level after 4 or 16 h of VPA treatment.

for genes bound by P300 than for unbound genes, both after 4 and 16 h of VPA treatment ($p \ll 10^{-10}$, two-tailed t test) (Fig. 3, *D* and *E*). Similar to DNase I-hypersensitive promoters, promoters bound by P300 also showed a significant increase in acetylation even at low initial acetylation levels (supplemental Fig. S6A). However, no significant difference between genes that were not bound by P300 to the entire set of genes was observed at different initial acetylation levels (supplemental

Fig. S6B), suggesting that other HATs are also involved in determining the initial H3K9ac level and affecting the response of the cells to HDAC inhibition. Taken together, these data suggest that the initial H3K9ac level at a given promoter influences the recruitment of P300 and other HATs to that promoter following HDAC inhibition (probably by conferring an accessible chromatin structure), thereby further increasing histone acetylation.

VPA-induced Genome-wide H3K9ac Patterns in ESCs

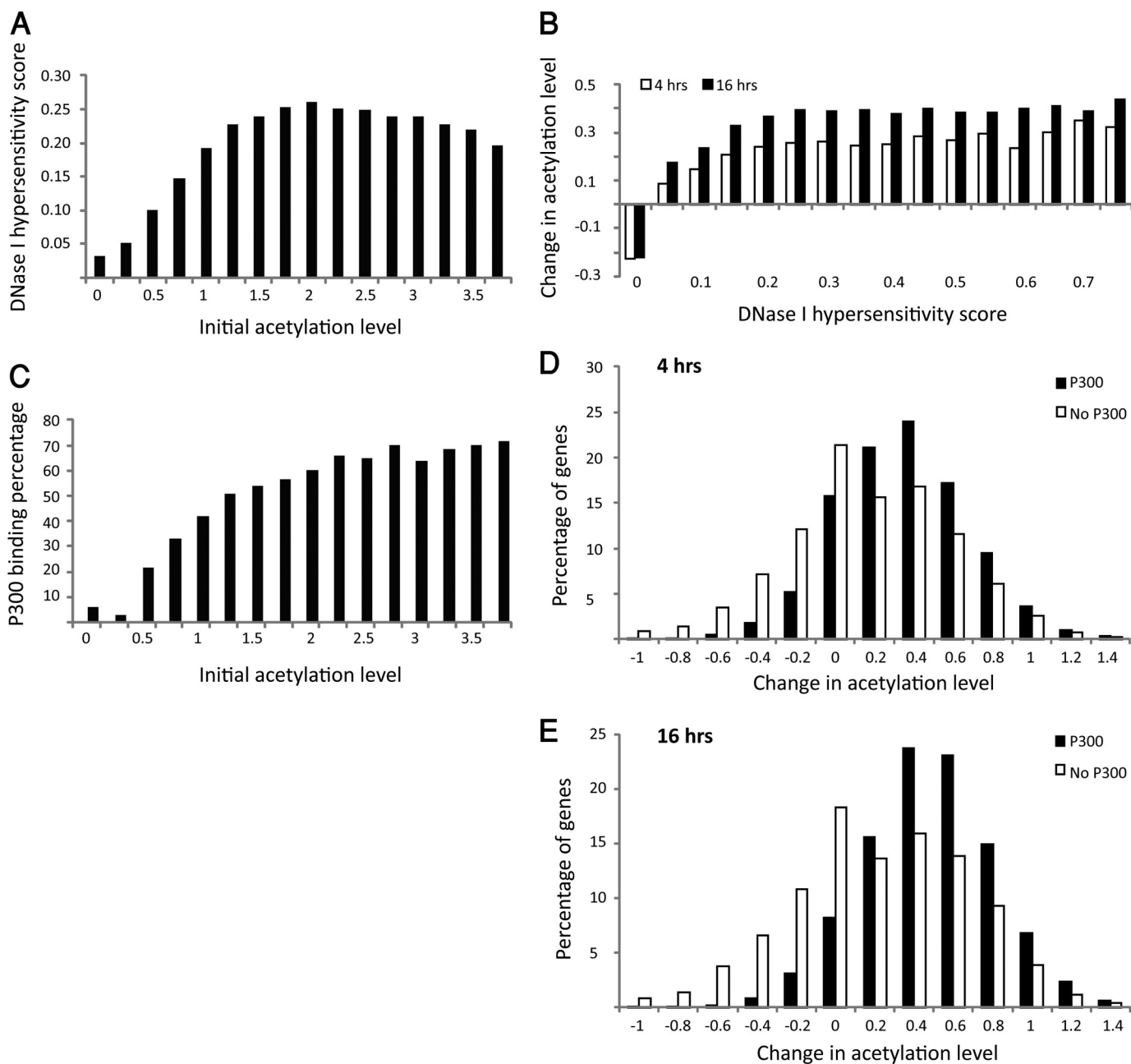


FIGURE 3. Sensitivity to DNase I and binding by P300 affect the response to HDAC inhibition. *A*, the average DNase I hypersensitivity score was calculated for the genes in each range of initial acetylation levels. Promoters that did not overlap with any DNase I-hypersensitive sites were regarded as genes with a DNase I hypersensitivity score of 0. *B*, genes were divided into 16 groups based on their DNase I hypersensitivity scores. The average change in acetylation enrichment score after either 4 or 16 h of VPA treatment was calculated for each group. Promoters that did not overlap any DNase I-hypersensitive sites were regarded as genes with a DNase I hypersensitivity score of 0. *C*, the percentage of genes with P300 peaks at their promoters (y axis) was calculated for each range of initial acetylation levels (x axis). *D* and *E*, distribution of P300 bound or unbound genes according to the change in the H3K9 acetylation level after 4 h (*D*) or 16 h (*E*) of VPA treatment.

Acetylation Level of H3K9 Correlates with Binding of Various Transcription Factors and Active Histone Modifications—In a previously published study (36), ChIP-seq was used to map the binding sites of 13 transcription factors and two transcription regulators in mouse ESCs, and *k*-means clustering was performed to generate five classes of genes, based on the binding patterns of these factors. Class I genes were enriched for binding by Nanog, Oct4, Sox2, Smad1, and STAT3; class II genes were bound by *c*-Myc and *n*-Myc; class III genes showed enrichment in binding by *n*-Myc, Klf4, Esrrb, Tcfcp2l1, Zfx, and

E2f1; class IV genes were enriched in Suz12-bound genes; and class V genes were deficient in all of these TFs. In order to identify a possible relationship between binding by these TFs, which are known to play different roles in ESC biology (36), and H3K9 acetylation and the response of different genes to HDAC inhibition, we compared the distribution of the five classes in genes with different initial H3K9ac levels. Although most of the genes that were not acetylated were also not bound by any TF (class V genes), most of the genes with high acetylation levels were bound by *c*-Myc and *n*-Myc

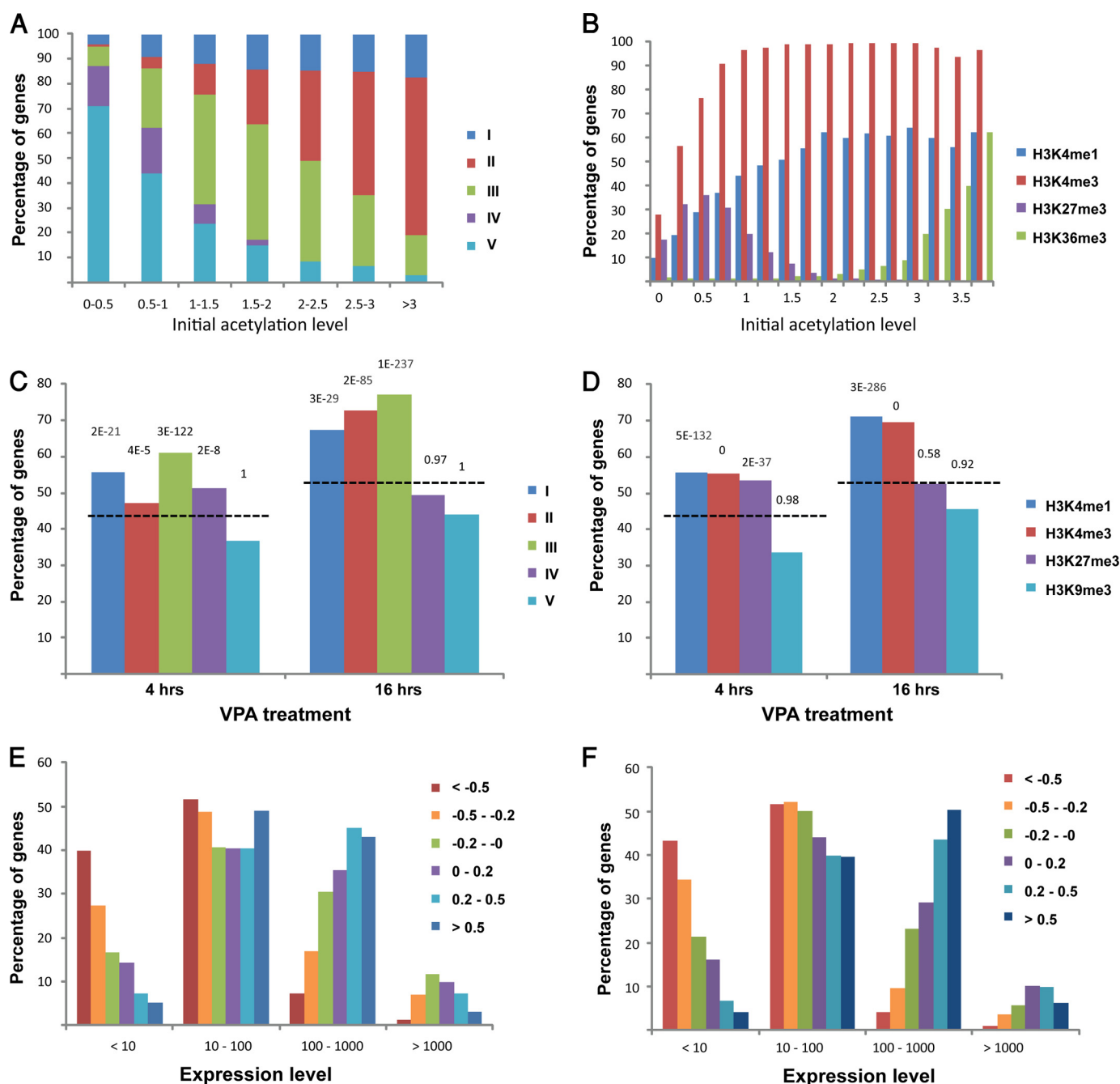


FIGURE 4. Acetylation level of H3K9 correlates with binding of transcription factors and active histone modifications. *A*, genes were divided into seven groups based on their initial H3K9 acetylation level. The distribution of the five gene classes generated by (36) was calculated for each range of initial acetylation levels. *B*, the percentage of genes whose promoters overlap with genomic regions enriched by different histone modifications was calculated for each range of initial acetylation levels. *C* and *D*, the percentage of genes whose H3K9 acetylation enrichment score increased by over 0.2 after 4 or 16 h of VPA treatment was calculated for genes of different classes (*C*) or for genes whose promoters overlap genomic regions enriched by different histone modifications (*D*). Dashed lines represent the percentage for the entire gene set. *p* values of Fisher's test for hypergeometric distribution are indicated above each column. *E* and *F*, histograms of gene expression levels are presented for genes with different levels of change in acetylation level of H3K9ac, after 4 h (*E*) or 16 h (*F*) of VPA treatment. The units of gene expression are log of the robust multiarray average-normalized expression values.

(class II genes) (Fig. 4A). The percentage of class I genes also increased with H3K9ac level, class IV genes (bound by Suz12) decreased with acetylation, and the percentage of class III genes was highest for genes with intermediate levels of acetylation. Similar correlation was observed between H3K9ac level and the percentage of promoters marked by the promoter-related histone marks H3K4me1 and H3K4me3 and the transcriptional elongation marker

H3K36me3, all previously mapped using ChIP-seq (28, 29) (Fig. 4B). When we examined the percentage of promoters that overlap regions enriched for H3K27me3, a repressive histone modification, we found that many genes with low H3K9ac level are also trimethylated on H3K27 (Fig. 4B). This is in agreement with a previous study that showed that certain lineage-specific genes are marked by H3K27me3 as well as H3K4me3 and H3K9ac (8).

VPA-induced Genome-wide H3K9ac Patterns in ESCs

To examine whether binding by various TFs and histone modifications affects the potential of promoters to display increased acetylation level following VPA treatment, we checked the percentage of promoters that increased in acetylation among classes of genes bound by different TFs (Fig. 4C) or promoters marked by different histone modifications (Fig. 4D) compared with the entire gene set. Classes I, II, and III were significantly enriched for genes with increased acetylation following HDAC inhibition compared with the entire gene set ($p < 4 \times 10^{-5}$, Fisher's test for hypergeometric distribution), whereas a lower percentage of genes became acetylated among class V than in the entire gene set (Fig. 4C). Similarly, promoters overlapping the active histone marks H3K4me1 and H3K4me3 were significantly enriched for genes with increased acetylation following HDAC inhibition compared with the entire gene set ($p \ll 10^{-10}$), whereas a lower percentage of genes became acetylated among promoters overlapping the heterochromatin-associated histone mark H3K9me3 (Fig. 4D). In agreement with these data, genes with significant increased H3K9 promoter acetylation levels after HDAC inhibition were expressed at higher levels than genes with unchanged or decreased acetylation level (Fig. 4, E and F).

Bivalent Promoters Restore HDAC Inhibitor-mediated Initial Increase in H3K9 Acetylation—Our data demonstrated that many promoters marked by H3K27me3 correspond to genes with very low levels of H3K9ac (Fig. 4B). To directly examine whether bivalent promoters are marked by H3K9ac, we checked the initial acetylation level of promoters previously found to be marked by both H3K4me3 and H3K27me3 in mouse ESCs (29). We found that most of the genes had very low levels of H3K9ac before the VPA treatment and that almost all of them were hyperacetylated following the treatment (Fig. 5, A and B). Unlike most of the genes, for which the response to HDAC inhibition was significantly stronger after 16 h than after 4 h ($p \ll 10^{-10}$, two-tailed *t* test) (Figs. 1B, 2E, and 5E), bivalent genes did not show a significant difference in the increase in acetylation level between 4 and 16 h ($p > 0.1$) (Fig. 5C). In many bivalent genes, the increase in acetylation was larger after 4 h than after 16 h (Fig. 5, A and D). Consistent with this, for genes bound by most of the TFs and histone modifications, the percentage of genes with increased acetylation was higher after 16 h than after 4 h of VPA treatment, whereas for genes marked by H3K27me3 or bound by Suz12 (a component of the repressive polycomb PRC2/EED-EZH2 complex, which methylates H3K27), the percentage was higher after 4 h than after 16 h (Fig. 4, C and D). These results indicate that the acetylation level of H3K9 in the promoters of bivalent genes increases transiently after HDAC inhibition but, unlike the rest of the acetylated genes, remains low or reverts back to the initial acetylation level. This phenomenon might imply a negative feedback response that acts to maintain low levels of H3K9 acetylation in promoters of bivalent genes in ESCs.

H3K9 Acetylation Level Predicts Different Cellular Locations—Because we saw that H3K9ac levels correlate with many biological processes, including gene expression, transcription factor binding, and histone modifications, we wished to functionally annotate genes with different initial levels of H3K9 acetylation. In order to do so, we used the DAVID functional

annotation tool (37, 38) to identify enriched gene ontology (GO) terms. The enriched terms are listed in [supplemental Table S2](#). In order to classify the cellular compartment-related terms into main classes (general cellular locations), we used the cateGORizer web tool (37). Curiously, we found that genes with different acetylation levels were enriched for different cellular compartments: genes with low acetylation levels were enriched for proteins located at the extracellular region and plasma membrane; genes with intermediate levels of acetylation were enriched for proteins located at different cytoplasm regions and organelles; and highly acetylated genes were enriched for proteins located at the ribosome, nucleus, and chromosome ([supplemental Fig. S7A](#)). Because H3K9ac levels are highly correlated with gene expression levels (Fig. 1C), we examined the cellular localization of gene products with different gene expression levels. This time, only two major groups were classified: lowly expressed genes were enriched for extra cellular region and plasma membrane, whereas highly expressed genes were enriched for cytoplasm, ribosome, nucleus, and chromosome ([supplemental Fig. S7B](#)). Next, we repeated the same analysis for two differentiated cell lines, MEFs and Met murine hepatocyte cells, using published microarray data sets (39, 40), and found a similar trend ([supplemental Fig. S7, C and D](#)). However, GO terms related to the chromosome and nucleus were shifted toward genes expressed at lower levels ([supplemental Fig. S7, C and D](#)), compared with ESCs ([supplemental Fig. S7B](#)). This might be due to the fact that the ESC genome is transcriptionally hyperactive (4, 41), which might require higher levels of gene expression for gene products that are localized in the nucleus and chromosomes.

To gain an insight into which biological pathways are affected by low level VPA in ESCs, we performed GO analysis for the gene categories that responded to VPA treatment after 4 h. We found some categories that suggest a general response to a drug, probably reflecting the cell's attempt to remove the drug. These included “vacuole,” “integral to membrane,” “lysosome,” “lytic vacuole,” and “intrinsic to membrane” ([supplemental Fig. S8](#)). Interestingly, in addition to this general response, we found a more specific set of categories, including “nucleosome assembly,” “chromatin assembly,” “nucleosome organization,” and “protein-DNA complex assembly” ([supplemental Fig. S8](#)), suggesting a chromatin-related response of the downstream responders to increased histone acetylation. It should be noted that the fact that the drug that caused these categories to respond is affecting chromatin by itself cannot explain these interesting results because the drug affects the acetylation state of the promoters of essentially all active genes and not the proteins themselves. Remarkably, 28 of the 77 genes (36%) that were found to be overexpressed following the 4-h VPA treatment were also enriched for H3K9ac in their promoters after the treatment ([supplemental Fig. S8B](#), $p = 0.009$), suggesting a direct effect of HDAC inhibition on these genes.

Decreased Expression of HDAC1 during ESC Differentiation—In order to identify key processes that regulate the early differentiation of mouse ESCs, we computed the activity score of 288 known pathways (from the Pathway Interaction Database, available on the World Wide Web) at 11 different time points during the differentiation of ESCs into EBs, based on gene

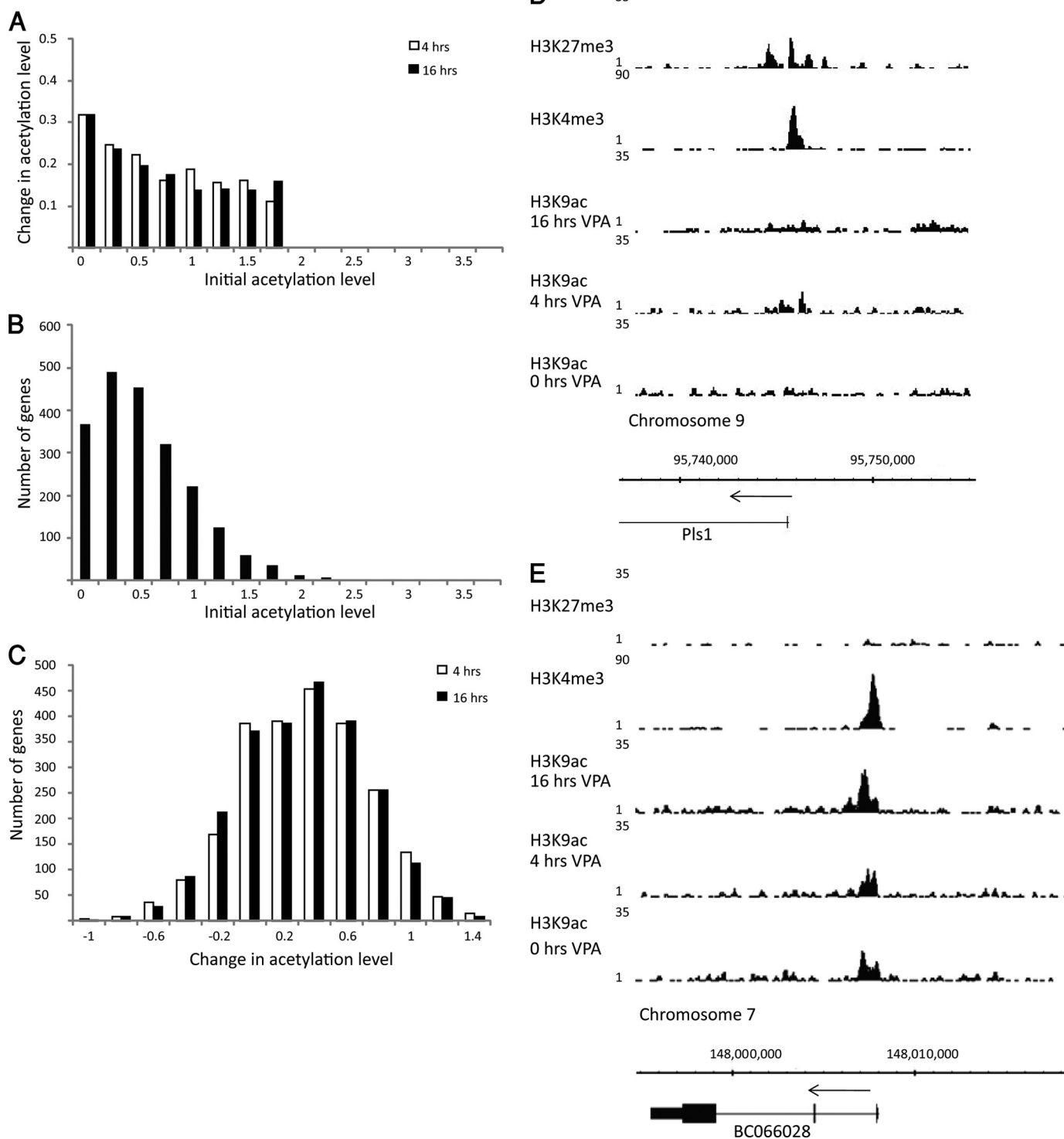


FIGURE 5. **Bivalent promoters transiently increase in acetylation following VPA treatment.** *A*, 2,373 bivalent genes were divided into 16 groups based on their initial H3K9 acetylation level. The average change in acetylation enrichment score after either 4 or 16 h of VPA treatment was calculated for each group. *B*, the number of genes in each initial H3K9 acetylation level. *C*, distribution of bivalent genes according to the change in the H3K9 acetylation level after 4 or 16 h of VPA treatment. *D* and *E*, signals of H3K27me3, H3K4me3, and H3K9ac in cells treated with VPA for 0, 4, or 16 h, around the TSS of a bivalent gene (*D*) and a gene with only H3K4me3 and no H3K27me3 (*E*).

expression microarray data sets of R1 and V6.5 mouse ESCs (34). The pathway that showed the most significant reduction in activity during the course of differentiation in both R1 and V6.5 cells was “signaling events mediated by HDAC class I” (supplemental Fig. S9A). The activity of this pathway decreased

during the first 96 h of differentiation in V6.5 cells and during the first 36 h in R1 cells.

In order to examine whether the expression levels of class I HDACs, the VPA substrates, change during differentiation, we looked for their expression in previously published microarray

VPA-induced Genome-wide H3K9ac Patterns in ESCs

data sets. We compared the expression levels of HDAC1, HDAC2, HDAC3, and HDAC8 in R1 cells and neuronal progenitor cells in whole genome tiling arrays (4) (supplemental Fig. S9B) and of HDAC1, HDAC2, and HDAC3 in undifferentiated ESCs and in 14-day-old EBs (supplemental Fig. S9C) from the same gene expression microarrays that were used for the calculation of the pathway activity scores (34). HDAC1 was highly abundant in ESCs, and its expression decreased following differentiation in all of the examined data sets, whereas the other class I HDACs showed lower expression levels, which did not change following differentiation (supplemental Fig. S9, B and C). In order to validate the down-regulation in HDAC1 expression, we measured the expression level of HDAC1 in R1 and E14 ESCs and in neuronal progenitor cells derived from R1 cells using real-time RT-PCR. HDAC1 expression decreased significantly following differentiation of ESCs into neuronal progenitor cells and was lower in E14 cells than in R1 cells (supplemental Fig. S9D). These results confirm the microarray data and suggest that HDAC1 is probably the main target of VPA and may have important roles in ESC maintenance and pluripotency (12).

DISCUSSION

In this study, we showed that treatment of E14 ESCs with low levels of VPA leads to a mild (20–40%) but a pervasive genome-wide increase in H3K9 acetylation level, albeit with very little effect on gene expression level. This might suggest that the increase in pluripotency following treatment with low levels of HDAC inhibitors (13) is, at least in part, due to a global effect. Chromatin in ESCs is distinguished from that of differentiated cells in its globally open structure, unique set of histone modifications, and looser binding (~20% difference) of architectural proteins (2, 4, 42), indicating that chromatin state might have a direct influence on pluripotency. H3K9ac is a histone modification associated with open chromatin, and it is enriched in ESCs compared with differentiated cells (4, 21, 27). It is possible that a global increase in the acetylation level of H3K9 leads to a small but meaningful shift of the chromatin state toward a more open conformation, which enables low level transcription throughout the genome, as observed in mouse R1 ESCs (4). In addition, although a global transcriptional response was not observed in response to low levels of VPA, the expression level of several genes did increase reproducibly following VPA treatment. For example, the expression level of a few different extracellular matrix-related genes (with enriched extracellular matrix-related GO categories) increased after 16 h of VPA treatment. We showed that simultaneous knockdown of two of these genes (*Acan* and *Col11a1*) leads to spontaneous differentiation, indicating that extracellular matrix may support the pluripotent, undifferentiated state (13). Other up-regulated genes might also have roles in increasing pluripotency following HDAC inhibition in yet unknown mechanisms.

Curiously, we found that several different properties increased the potential of gene promoters to be hyperacetylated following HDAC inhibition. These properties included hypersensitivity to DNase I digestion and to binding of P300 and of different pluripotency-related transcription factors and active histone marks. All of these properties characterize regions of

open and accessible chromatin. Promoters that are not sensitive to DNase I digestion, are not bound by any transcription factors, and are marked by repressive histone marks (*i.e.* H3K9me3) did not tend to be hyperacetylated following HDAC inhibition. This suggests that HDAC inhibition alone is not sufficient to elevate the acetylation level of specific genomic regions, but recruitment of HATs to these regions is also required.

The decrease in acetylation level observed in many genes following HDAC inhibition, most of them characterized by condensed chromatin properties, implies the existence of a feedback mechanism that acts to maintain a constant acetylation level across the genome. In the majority of the genes, the existence of such a mechanism is insufficient to prevent elevation in histone acetylation but might decrease the degree of elevation. However, in specific genes, it might lead to a decrease in acetylation level following HDAC inhibition. For example, in genes with extremely high levels of H3K9 acetylation, the level of acetylation decreased after 4 h and increased very mildly (by less than 5% on average) after 16 h of VPA treatment. This might result from the relative depletion of HDAC binding in the promoters of these genes. In such cases, HDAC inhibition would not have an effect on acetylation level, and feedback mechanisms might decrease acetylation. Another group of genes in which it is apparent that feedback mechanisms play an important role is bivalent genes, which are marked by H3K4me3 and H3K27me3 (8, 9). Although in the promoters of most genes the increase in H3K9 acetylation was proportional to the time of treatment, increasing considerably between 4 and 16 h, implying a lack of a dominant acetylation-restraining mechanism, in the promoters of bivalent genes, the acetylation level did not increase between 4 and 16 h, and in some genes it even decreased at the 16 h time point. Because many of these genes are known to have developmental functions and are required to remain silent in undifferentiated ESCs (8, 9), it seems possible that a unique mechanism exists that acts to maintain low levels of H3K9 acetylation in the promoters of these bivalent genes in order to prevent their expression.

In contrast to H3K9 acetylation levels, which increased globally across the genome over time following VPA treatment, the number of up-regulated genes after 4 h of VPA treatment was about twice the up-regulated genes after 16 h, demonstrating a transient and limited increase in gene expression. This suggests the presence of a compensating mechanism that restrains changes in gene expression following HDAC inhibition. One such potential mechanism could be the down-regulation of KAT2B, a histone H3 lysine acetyltransferase that is a part of several complexes that function as transcriptional activators (43). The down-regulation of KAT2B may act to specifically reduce the acetylation and expression of genes that were overexpressed after 4 h. Such a mechanism could also contribute to the uncoupling observed between hyperacetylation and gene expression following VPA treatment. Despite the strong correlation between acetylation and gene expression before the treatment, the global pervasive increase in acetylation did not result in significant pervasive changes in gene expression. This is in agreement with recent studies that showed that global increase in histone methylation did not correspond to changes

in gene expression (44, 45). Such uncoupling between changes in histone modifications and gene expression might imply that elevation of a single histone modification is insufficient to significantly alter gene expression and that the complexity of the different histone modifications acts redundantly as a buffer to ensure proper gene regulation. However, it could also result from feedback mechanisms that affect gene expression to a larger extent than they affect histone modifications.

Examination of promoters with gradually increasing initial levels of H3K9 acetylation revealed gradual and progressive changes of different genomic features, including an increase in DNase I hypersensitivity, an increase in the binding of P300 and several transcription factors, a decrease in the binding of the polycomb protein Suz12, and an increase in active histone marks. Although the correlation between H3K9 acetylation level and other features associated with open chromatin is not surprising by itself, the gradual and “smooth” nature of the data is remarkable. Perhaps most surprising is the prominent difference in enrichment of cellular compartment GO terms in genes with different initial acetylation levels (supplemental Fig. S7). The transition from GO categories related to the external cellular regions to categories related to the internal part of the nucleus was also gradual in nature. The fact that H3K9 acetylation level determines different cellular properties supports the idea that this modification has an important role in ESC biology (13).

To summarize, in this study, we generated genome-wide maps of H3K9ac in ESCs grown under normal conditions and characterized the changes occurring in H3K9 acetylation level after treating the cells with low levels of VPA for two different incubation times. We showed a global increase in the acetylation level of H3K9 following HDAC inhibition and identified several genes that are responsive to low levels of VPA. We also demonstrated that the compaction of the chromatin and the binding of P300 affect the response of different promoters to HDAC inhibition. Promoters surrounded by open chromatin regions and bound by P300 tended to be more prone to hyperacetylation following VPA treatment. Regardless, a specific mechanism seems to operate to selectively prevent hyperacetylation of bivalent genes. These findings shed light on the molecular processes occurring in E14 ESCs in response to HDAC inhibition and suggest that H3K9 acetylation level is correlated with pluripotency.

Acknowledgments—We thank members of our laboratory for critical comments and Michal Bronstein and Mira Korner from the Center for Genomic Analysis of the Hebrew University.

REFERENCES

- Gaspar-Maia, A., Alajem, A., Meshorer, E., and Ramalho-Santos, M. (2011) *Nat. Rev. Mol. Cell Biol.* **12**, 36–47
- Meshorer, E., Yellajoshula, D., George, E., Scambler, P. J., Brown, D. T., and Misteli, T. (2006) *Dev. Cell* **10**, 105–116
- Aoto, T., Saitoh, N., Ichimura, T., Niwa, H., and Nakao, M. (2006) *Dev. Biol.* **298**, 354–367
- Efroni, S., Dutttagupta, R., Cheng, J., Dehghani, H., Hoepfner, D. J., Dash, C., Bazett-Jones, D. P., Le Grice, S., McKay, R. D., Buetow, K. H., Gingeras, T. R., Misteli, T., and Meshorer, E. (2008) *Cell Stem Cell* **2**, 437–447
- Kobayakawa, S., Miiike, K., Nakao, M., and Abe, K. (2007) *Genes Cells* **12**, 447–460
- Mattout, A., and Meshorer, E. (2010) *Curr. Opin. Cell Biol.* **22**, 334–341
- Meshorer, E., and Misteli, T. (2006) *Nat. Rev. Mol. Cell Biol.* **7**, 540–546
- Azuara, V., Perry, P., Sauer, S., Spivakov, M., Jørgensen, H. F., John, R. M., Gouti, M., Casanova, M., Warnes, G., Merckenschlager, M., and Fisher, A. G. (2006) *Nat. Cell Biol.* **8**, 532–538
- Bernstein, B. E., Mikkelsen, T. S., Xie, X., Kamal, M., Huebert, D. J., Cuff, J., Fry, B., Meissner, A., Wernig, M., Plath, K., Jaenisch, R., Wagschal, A., Feil, R., Schreiber, S. L., and Lander, E. S. (2006) *Cell* **125**, 315–326
- Shahbazian, M. D., and Grunstein, M. (2007) *Annu. Rev. Biochem.* **76**, 75–100
- Lagger, G., O’Carroll, D., Rembold, M., Khier, H., Tischler, J., Weitzer, G., Schuettengruber, B., Hauser, C., Brunmeir, R., Jenuwein, T., and Seiser, C. (2002) *EMBO J.* **21**, 2672–2681
- Dovey, O. M., Foster, C. T., and Cowley, S. M. (2010) *Proc. Natl. Acad. Sci. U.S.A.* **107**, 8242–8247
- Hezroni, H., Tzchori, I., Davidhi, A., Mattout, A., Biran, A., Nissim-Rafinia, M., Westphal, H., and Meshorer, E. (2011) *Nucleus* **2**, 300–309
- Lee, J. H., Hart, S. R., and Skalnik, D. G. (2004) *Genesis* **38**, 32–38
- Ware, C. B., Wang, L., Mecham, B. H., Shen, L., Nelson, A. M., Bar, M., Lamba, D. A., Dauphin, D. S., Buckingham, B., Askari, B., Lim, R., Tewari, M., Gartler, S. M., Issa, J. P., Pavlidis, P., Duan, Z., and Blau, C. A. (2009) *Cell Stem Cell* **4**, 359–369
- Karantzali, E., Schulz, H., Hummel, O., Hubner, N., Hatzopoulos, A., and Kretsovali, A. (2008) *Genome Biol.* **9**, R65
- Zhou, Q. J., Xiang, L. X., Shao, J. Z., Hu, R. Z., Lu, Y. L., Yao, H., and Dai, L. C. (2007) *J. Cell. Biochem.* **100**, 29–42
- Huangfu, D., Maehr, R., Guo, W., Eijkelenboom, A., Snitow, M., Chen, A. E., and Melton, D. A. (2008) *Nat. Biotechnol.* **26**, 795–797
- Huangfu, D., Osafune, K., Maehr, R., Guo, W., Eijkelenboom, A., Chen, S., Muhlestein, W., and Melton, D. A. (2008) *Nat. Biotechnol.* **26**, 1269–1275
- Bártová, E., Galiová, G., Krejčí, J., Harnicarová, A., Strasák, L., and Kozubek, S. (2008) *Dev. Dyn.* **237**, 3690–3702
- Krejčí, J., Uhlířová, R., Galiová, G., Kozubek, S., Smigová, J., and Bártová, E. (2009) *J. Cell. Physiol.* **219**, 677–687
- Langmead, B., Trapnell, C., Pop, M., and Salzberg, S. L. (2009) *Genome Biol.* **10**, R25
- Xu, H., Handoko, L., Wei, X., Ye, C., Sheng, J., Wei, C. L., Lin, F., and Sung, W. K. (2010) *Bioinformatics* **26**, 1199–1204
- Blankenberg, D., Von Kuster, G., Coraor, N., Ananda, G., Lazarus, R., Mangan, M., Nekrutenko, A., and Taylor, J. (2010) *Curr. Protoc. Mol. Biol.*, Chapter 19, 10, 11–21
- Ye, T., Krebs, A. R., Choukallah, M. A., Keime, C., Plewniak, F., Davidson, I., and Tora, L. (2011) *Nucleic Acids Res.* **39**, e35
- Shin, H., Liu, T., Manrai, A. K., and Liu, X. S. (2009) *Bioinformatics* **25**, 2605–2606
- Creyghton, M. P., Cheng, A. W., Welstead, G. G., Kooistra, T., Carey, B. W., Steine, E. J., Hanna, J., Lodato, M. A., Frampton, G. M., Sharp, P. A., Boyer, L. A., Young, R. A., and Jaenisch, R. (2010) *Proc. Natl. Acad. Sci. U.S.A.* **107**, 21931–21936
- Meissner, A., Mikkelsen, T. S., Gu, H., Wernig, M., Hanna, J., Sivachenko, A., Zhang, X., Bernstein, B. E., Nusbaum, C., Jaffe, D. B., Gnirke, A., Jaenisch, R., and Lander, E. S. (2008) *Nature* **454**, 766–770
- Mikkelsen, T. S., Ku, M., Jaffe, D. B., Issac, B., Lieberman, E., Giannoukos, G., Alvarez, P., Brockman, W., Kim, T. K., Koche, R. P., Lee, W., Mendenhall, E., O’Donovan, A., Presser, A., Russ, C., Xie, X., Meissner, A., Wernig, M., Jaenisch, R., Nusbaum, C., Lander, E. S., and Bernstein, B. E. (2007) *Nature* **448**, 553–560
- Zhang, Y., Liu, T., Meyer, C. A., Eickhout, J., Johnson, D. S., Bernstein, B. E., Nusbaum, C., Myers, R. M., Brown, M., Li, W., and Liu, X. S. (2008) *Genome Biol.* **9**, R137
- Efroni, S., Schaefer, C. F., and Buetow, K. H. (2007) *PLoS ONE* **2**, e425
- Hailesellasse Sene, K., Porter, C. J., Palidwor, G., Perez-Iratxeta, C., Muro, E. M., Campbell, P. A., Rudnicki, M. A., and Andrade-Navarro, M. A. (2007) *BMC Genomics* **8**, 85
- Schaefer, C. F., Anthony, K., Krupa, S., Buchoff, J., Day, M., Hannay, T., and Buetow, K. H. (2009) *Nucleic Acids Res.* **37**, D674–D679
- Glover, C. H., Marin, M., Eaves, C. J., Helgason, C. D., Piret, J. M., and

VPA-induced Genome-wide H3K9ac Patterns in ESCs

- Bryan, J. (2006) *PLoS Comput. Biol.* **2**, e158
35. Schnetz, M. P., Handoko, L., Akhtar-Zaidi, B., Bartels, C. F., Pereira, C. F., Fisher, A. G., Adams, D. J., Flicek, P., Crawford, G. E., Laframboise, T., Tesar, P., Wei, C. L., and Scacheri, P. C. (2010) *PLoS Genet.* **6**, e1001023
36. Chen, X., Xu, H., Yuan, P., Fang, F., Huss, M., Vega, V. B., Wong, E., Orlov, Y. L., Zhang, W., Jiang, J., Loh, Y. H., Yeo, H. C., Yeo, Z. X., Narang, V., Govindarajan, K. R., Leong, B., Shahab, A., Ruan, Y., Bourque, G., Sung, W. K., Clarke, N. D., Wei, C. L., and Ng, H. H. (2008) *Cell* **133**, 1106–1117
37. Hu, Z. L., Bao, J., and Reecy, J. M. (2008) *Online J. Bioinformatics* **9**, 108–112
38. Huang da, W., Sherman, B. T., and Lempicki, R. A. (2009) *Nucleic Acids Res.* **37**, 1–13
39. Conigliaro, A., Colletti, M., Cicchini, C., Guerra, M. T., Manfredini, R., Zini, R., Bordoni, V., Siepi, F., Leopizzi, M., Tripodi, M., and Amicone, L. (2008) *Cell Death Differ.* **15**, 123–133
40. Sridharan, R., Tchieu, J., Mason, M. J., Yachechko, R., Kuoy, E., Horvath, S., Zhou, Q., and Plath, K. (2009) *Cell* **136**, 364–377
41. Efroni, S., Melcer, S., Nissim-Rafinia, M., and Meshorer, E. (2009) *Cell Cycle* **8**, 43–48
42. Boyer, L. A., Plath, K., Zeitlinger, J., Brambrink, T., Medeiros, L. A., Lee, T. I., Levine, S. S., Wernig, M., Tajonar, A., Ray, M. K., Bell, G. W., Otte, A. P., Vidal, M., Gifford, D. K., Young, R. A., and Jaenisch, R. (2006) *Nature* **441**, 349–353
43. Nagy, Z., and Tora, L. (2007) *Oncogene* **26**, 5341–5357
44. Jiang, H., Shukla, A., Wang, X., Chen, W. Y., Bernstein, B. E., and Roeder, R. G. (2011) *Cell* **144**, 513–525
45. Koche, R. P., Smith, Z. D., Adli, M., Gu, H., Ku, M., Gnirke, A., Bernstein, B. E., and Meissner, A. (2011) *Cell Stem Cell* **8**, 96–105